Hot Electron Detection
In Intense Laser-Plasma Interactions

Asher Davidson
Mentor: Christoph Niemann

Our experimental group develops methods to detect high-energy electrons produced by laser-plasma instabilities. These electrons, which range up to hundreds of keV, prove a major challenge for inertial confinement fusion (such as at NIF). They can preheat fuel, resulting in more energy being required to compress fuel to the point of ignition. We concentrated a laser (to an intensity of $10^{13} \sim 10^{14} W/cm^2$) on various targets, exciting them into a plasma state, then built and tested detection mechanisms for the emitted electrons.

I. INTRODUCTION

Laser-Plasma interactions are of interest to scientists for their implications with Inertial Confinement Fusion (ICF). In ICF, fusion is attempted by compressing a fuel pellet to a density comparable to the center of a star. This compression is done by the force of a direct or indirect radiation from a laser. The laser will typically excite the materials in the region into a plasma state, the plasma then interacting with the incoming laser. The interaction produces high energy electrons witch heat the fuel before it has been sufficiently compressed. The adiabatic property of the heated fuel changes, making it require more energy to be applied for sufficient compression. It is of great interest to laser-fusion laboratories, such as NIF, to minimize this effect in order to successfully ignite the fuel[1, 2].

Plasmas are notorious for their highly nonlinear nature. Predicting laser-plasma interaction is impossible to do analytically, and difficult to do numerically. Computational models' effectiveness must first be verified with experimental results. It is therefore important to develop sophisticated experimental methods for directly observing the emitted electrons. Our goal is to develop detectors with witch we can observe the spatial, temporal, and spectral dependence of the hot electrons.

In Section II: THEORY I briefly cover the basic physics behind laser-plasma interactions. In Section III: EXPERIMENTAL DESIGN I present each of the three experiments we conducted during my stay at UCLA. In Section IV: RESULTS I present and explain the findings from the experiments described in Section III. Finally, I conclude everything in Section V: CONCLUSION.

II. THEORY

In laser-plasma interactions the electrons in the plasma couple with the fields in the laser in complicated ways, resulting in high nonlinearity. As a result it is impossible to find analytical solutions to real-world problems, and even difficult to build numerical simulations. Still, many important concepts arise from the theory, all important for anyone building an experimental apparatus involving such interactions. I will here present some theoretical facts and terminologies which are relevant to our experiments.

In an idealized model where the laser has a perfect Gaussian pulse, and all interactions are with the plasma (as opposed to other gases or materials that one might find in an experimental apparatus), the dispersion relation can be given by the following equation[3]:

$$\kappa c = \sqrt{\omega_{pe}^2/\gamma - \omega_o^2}$$

$$\omega_{pe} = \sqrt{4\pi n_e e^2/m_e}$$

The gamma term is the familiar term from relativity $\gamma = 1/\sqrt{1 - v^2/c^2}$, and ω_o is the frequency of the incident laser, and is equal to 1 in most applications. ω_{pe} is called the "quiver velocity", and is the frequency at

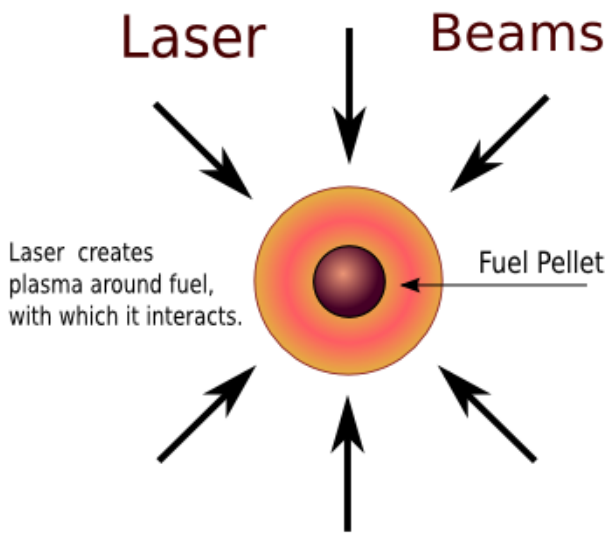

FIG. 1: The basic schematic of Inertial Confinement Fusion. Intense lasers are used to compress a spherical fuel pellet to the density comparable to the core of a star. The inertial of the fuel alone is sufficient to confine the fuel until ignition ensues. The laser, though, produces a plasma around the fuel with which it interacts. This interaction is the main concern of our plasma group.

which the electrons oscillate due to the electromagnetic fields associated with the incident laser. When the quiver velocity equals the incident laser frequency, the propagation vector approaches zero. When this happens, all of the incident laser is reflected off the plasma, after penetrating a distance denoted the "skin depth". The plasma density necessary for this to happen (called the critical density) is given by[3]:

$$n_{cr}\gamma\frac{1.1\times10^{21}}{\lambda_\mu}cm^{-3}$$

Where λ_μ is the incident wavelength given in micrometers. The critical density is very important in experimental plasma physics. If by some accident the plasma is compressed to this density, the incident beam may be reflected back into the laser, damaging the device. Even when the plasma is initially below the critical density, its surface may be "plowed" to this point by the pressure of the incident beam. Then density of the plasma can also affect how much of the energy is absorbed by the plasma and released in the form of hot electrons.

The most thoroughly understood laser-plasma interaction is the Inverse Bremsstrahlung. As the name indicates, it is opposite to what happens in a typical Bremsstrahlung (when an electron stops and produces a photon to conserve momentum). The incident photons here are absorbed by the electrons, speeding them up. The sped up electrons then collide with other electrons and ions, heating the plasma. The heating of the plasma results in an emission of electrons. The absorption coefficient of the plasma can be given by the equation:

$$\kappa\propto\frac{Zn_e^2}{T_e^{3/2}(1-n_e/n_{cr})^{1/2}}$$

An important consequence of this equation is that the absorption (and therefore the Inverse Bremsstrahlung effect in general) is most significant for plasmas of high-Z, high density, and low temperature. Unless the laser is able to heat the plasma to temperatures where other instabilities dominate, the Inverse Bremsstrahlung is the most significant source of emitted electrons.

When the laser is intense enough to heat the plasma significantly, the plasma may actually start resonating with the laser[4, 5]. This is called Stimulated Raman Scattering (SRS). This effect is proportional to the square root of the temperature, and in practice becomes significant at laser intensities of about $10^{14}W/cm^2$. Interestingly, this effect cannot occur above 1/4 of the critical density, due to the plasma reflecting too much of the laser. SRS is dominant in most inertial confinement facilities, such as at NIF. It is capable of producing electrons of extremely high energy, and can preheat the fuel before it has been sufficiently compressed. In order for Inertial Confinement Fusion to succeed, SRS has to be minimized as much as possible.

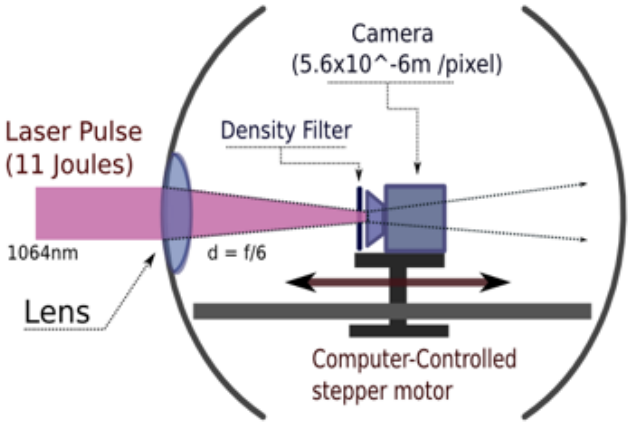

FIG. 2: This is the setup used to measure the width of the laser focus. The laser is focused by an F6 lens. A smaller value of F would mean a smaller focal width (and greater intensity), but a shorter length of focus. The stepper motor can be used to move the camera forwards and backwards.

III. EXPERIMENTAL DESIGN

I performed three different experiments, each contributing to the overall goal of developing and testing hot electron detectors. In order to test hot electron detectors, we needed to concentrate a high-energy laser onto a target inside a vacuum chamber. We used the PHOENIX laser at UCLA for all of our experiments (1064nm laser with pulse length of 5ns and 4GW of power).

The first of my experiments involved measuring the intensity of the laser at the focal point. The laser intensity determines what laser-plasma interaction dominates. We specifically wanted to reach an intensity of $10^{14}W/cm^2$ in order to observe Stimulated Raman Scattering. In the second experiment, we built Faraday cup detectors, and used them to observe the spatial resolution of electrons (and positive ions) around He plasma. Finally, I built an electron gun with which to calibrate an electron spectrometer, which we hope to use in the near future.

A. Laser Intensity

Figure 2 describes the experimental setup with which I measured the laser intensity. The basic premise was to mount a filter-protected camera to a computer-controlled stepper motor. We could scan along the laser and determine the minimum diameter (waist length) along the focus. In order to avoid saturating the camera, the laser was operated at the lowest possible power. A typical camera shot is shown in Figure 3. The diameter can be measured by taking the profile of the picture across the middle, and measuring the number of pixels across the FWHM (the brightness is measured from 0-256 bits).

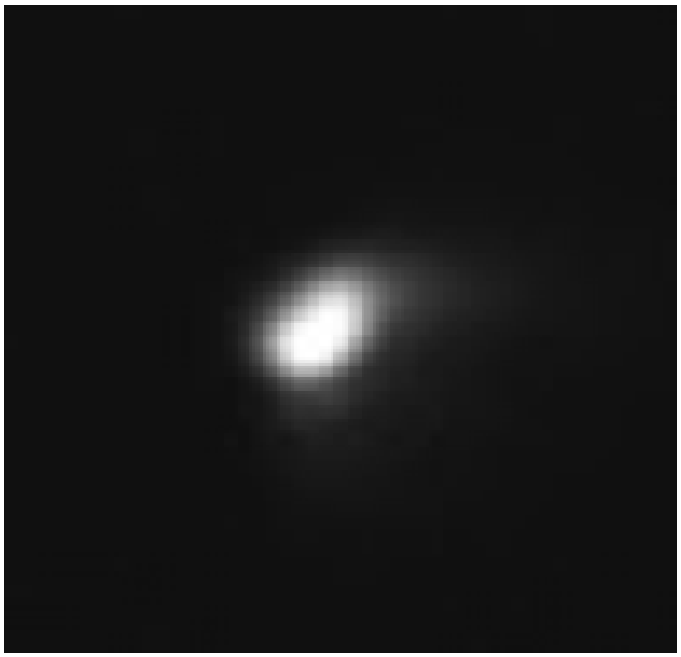

FIG. 3: This is a typical picture of the focal spot. It is slightly deformed, since the laser is operating at the lowest possible power. Each pixel is $5.6\mu m$ in width and height.

In order to measure the laser intensity, we also needed to know the peak laser power. The pulse shape of each shot could be measured by a photodiode detector attached to the oscilloscope. The voltage output of the detector is proportional to the power of the laser at that point in time. The pulse shape for one of our shots is shown in Figure 7. We knew from previous calibrations that the laser fired a total energy of 11 Joules. By dividing this value by the total area under the voltage-time plot, we determined the proportionality of the voltage to the power (which is energy per unit time). We then multiplied the peak voltage value with this proportionality constant to find the peak power of the laser shot, then calculated the peak laser intensity by dividing the peak laser power by the focal width obtained from setup 2.

The analysis of the experimental measurements is presented in part A of the results section of this report. The most important result of this measurement was that our laser intensity was in the $10^{13} W/cm^2$ range, just short of what was necessary to observe Stimulated Raman Scattering. Inverse Bremsstrahlung, which dominates at this intensity, is responsible for all of the hot electron data acquired during my stay at UCLA.

B. Spatial Resolution of e^-

Our main goal was to build and test detectors which could be used to determine the temporal, spatial, and spectral resolution of hot electrons. One of the simplest detectors we could build and use was the Faraday cup. The basic design of the detector is shown on Figure 4. It is composed of two main parts: a cylindrical aluminum wall, and a smaller brass cup located inside the wall. The two components are isolated by a plastic o-ring, but are both connected to the end of an AMS cable. The other end of the cable is connected to an oscilloscope. The aluminum wall has a circular hole on the end opposite to the brass cup. When electrons (or ions of any type) enter through this hole and reach the cup, charge builds up between the aluminum and the brass. The configuration charges like a capacitor, which then discharges through the oscilloscope's internal resistor. The oscilloscope can measure the voltage drop across the Faraday cup, giving insight into the rate at which the cup is gathering charged ions.

One of the biggest advantages of the Faraday cup is that it is easy to build; the aluminum cylinder and the brass cup can easily be manufactured with a lathe. We built two of our own Faraday cups for further experiments. Since they are so easy to build, they are easily configurable for specific experiments and setups. The Faraday cups that we built were of a conveniently small size, enabling us to easily relocate them inside our vacuum plasma chamber. By obtaining data at various locations, it is possible to acquire a spatial resolution of the electrons.

Still, the Faraday cup has some disadvantages when used on its own. A plasma typically emits positive ions as well as electrons. Any negative charge buildup in the cup due to an electron can be countered by collecting an equivalent number of positive ions. The net effect is that the detector measures the ratio of electrons to positive ions. A pulse of negative voltage will show that the cup is detecting electrons, but it is difficult to determine exactly how many electrons that pulse corresponds to. It might be detecting only a small number of electrons with no ions, or a very large number of electrons with many ions.

That being said, Faraday cups are still extremely useful for acquiring information about the electrons and ions emitted by a plasma. We proceeded to use these Faraday cups to determine the spatial resolution of the emission from a He plasma. The general setup of the experiment is shown in Figure 5. We placed a Faraday cup at each end of a long metal stand, facing each other. The stand was placed on a stepper motor capable of rotating to any desired position. In the middle of the gas chamber, in between the two Faraday cups, was a He gas jet. The gas jet was synchronized with the laser, such that it would fire a pulse of He gas at the moment the laser fired. The laser would then heat the He to a plasma, and exhibit various laser-plasma effects. The Faraday cups could be rotated to detect the electron/ion emissions from various angles. Conveniently, since there are two Faraday cups, we could obtain data at two opposite angles at the same time. Using this setup we observed the angular resolution of the election/ion radiation.

Our acquired data and the subsequent analysis will be covered in part B of the results section.

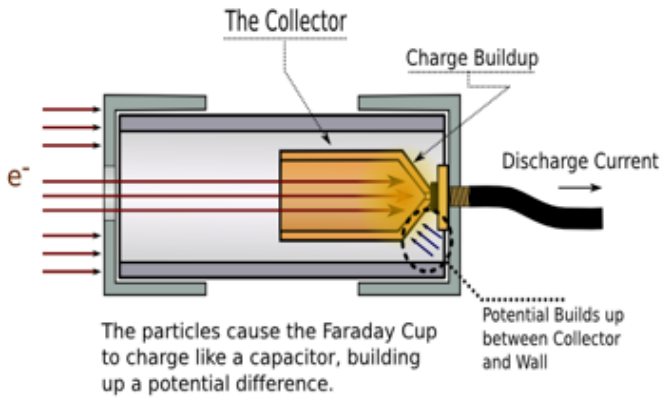

FIG. 4: This illustrates the workings of a typical Faraday cup. The Faraday cup is composed of a cylindrical aluminum wall on the outside, and a brass cup on the inside. The electrons (and ions) come in through a hole on one side of the cylinder, and are absorbed by the brass on the other side. The brass builds up in charge, and a potential drop across the cup and the wall results. This potential drop can be observed through an oscilloscope. The Faraday cup discharges across the oscilloscope's internal resistor, allowing for a rough temporal resolution.

C. Calibration of e^- Spectrometer

Another detector we worked with is the Concentric Hemispherical Analyzer (CHA), which is effectively an electron spectrometer. The design is shown in Figure 6. It consists of two conducting shells set at opposite potentials. Only electrons of specific energy will be deflected the amount necessary by the electric field to reach the detector on the other side (a Faraday cup or a photodiode). As a result of the geometry, the electrons coming in from one side of the CHA will be mapped to exactly the same location on the other side of the CHA. No ions will be able to pass through, since they will be deflected directly towards the walls.

The energy at which the electron is allowed to pass through to the detector is proportional to the potential applied to the two hemispheres. By varying this voltage, it is possible to acquire detailed spectral data of the electrons. The geometry specifies that the electron energy should be approximately four times the potential applied to the sides. Still, the proportionality may be slightly different from what is expected, and therefore needs to be measured directly. The proportionality can be determined by firing electrons of known energies into the CHA and determining at what voltage they can be detected. In order to calibrate the detector in this way, we needed to build an electron gun capable of firing electrons with controlled energy values.

Figure 15 shows the design of the electron gun we built. It is a naked light-bulb filament powered by a 9V battery and floating at a high voltage. The battery and the adjustable potentiometer are both located in a conducting box. The box is screwed to the grounded wall of the vacuum laser chamber, and also contains two feed-through rods entering the vacuum chamber and one for the high-voltage supply. The light-bulb filament is located inside the vacuum, and is connected to both the feed-throughs. The resistors in parallel and in series with the filament are there to make the current more gradually adjustable (the 10k pot has such a high resistance that without these resistors it acts like an on-off switch). The battery drives a current through the filament, heating it up. The heat of the filament will cause it to expel some electrons, which will then be propelled outwards by the strong negative voltage. A grounded plate with a small hole is placed in front of the filament. The electrons, repelled by the negative voltage and attracted to the ground, will fire towards the plate. The electrons that make it through the hole will then form a beam, each with precisely the energy corresponding to the voltage drop across the filament and the plate (times the charge of the electron).

The successes and problems of the electron gun, as well as possible improvements, will be discussed on part C of the results section.

IV. RESULTS

A. Laser Intensity

From the image profiles obtained from setup 2, we determined the minimum pulse width to be about $w_0 = 1.4 \times 10^{-4} m$. In order to verify that our measurements were reasonable, we plotted the width with respect to time. Theoretically, the laser width should disperse even as it is focused. Instead of focusing to a point, therefore, the laser width evens out at w_0, measured earlier. The width should roughly follow the following function (z is the distance from the focal point):

$$w(t) = w_0(1 + (\frac{\lambda z}{\pi w_0^2})^2)^{1/2}$$

The theoretical distribution of width is plotted alongside the measured values in Figure 8. They are reasonably close, although the experimental values trail off at large distances. When the Phoenix laser is set at lowest intensity (to avoid saturating the camera), it is unable to fire a perfectly circular shot. This deformity in the focal shape becomes significant at larger distances, making it difficult to determine its size. Near the focus, though, the laser shot is reasonably circular, and consistent with our expectation.

From the photodiode data in Figure 2, we found that the peak laser power was $P_{peak} = 1.3GW$. The maximum intensity of the laser is simply $I_{max} = P_{peak}/\pi(w_0/2)^2$. We found that the intensity of our laser was on the order of $8 \times 10^{13} W/cm^2$, just short of the $10^{14} W/cm^2$ range, which is what we needed to observe Stimulated Raman Scattering.

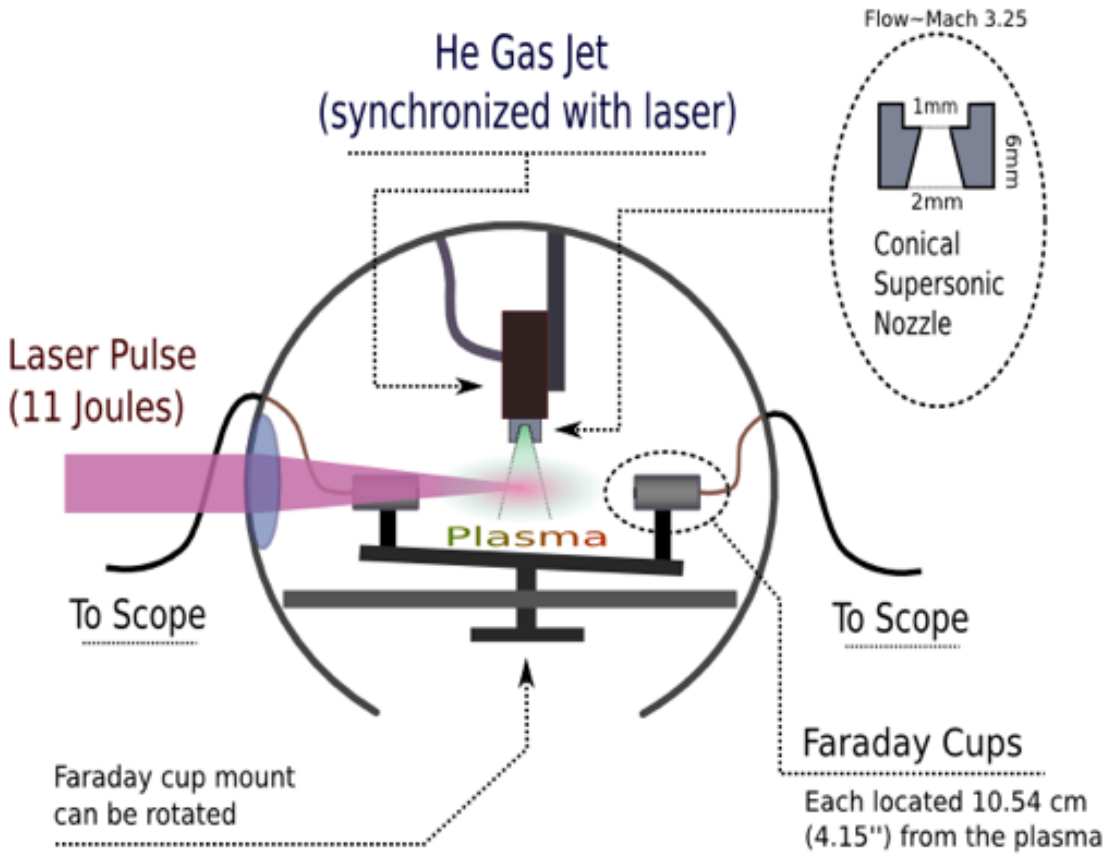

FIG. 5: We mounted a Faraday cup to the two ends of a long, metal stand. Each Faraday cup was located 10.5 cm from the plasma. The cups were set to face each other, both facing the plasma at the center. A He gas jet was set to synchronize with the laser so that it would supply the He plasma source. The stand may be rotated in order to obtain the electron/ion spectrum taken from various angles.

One reason for the low intensity is that a capacitor for one of the PHOENIX laser amplifiers was malfunctioning. Replacing this amplifier would allow the laser to reach intensities sufficient to observe SRS. Unfortunately, the capacitor could not be replaced within the time I was at UCLA. Inverse Bremsstrahlung is the laser-plasma instability that dominates in these low-intensity regions, and is therefore responsible for the hot electron data I acquired during my time at UCLA.

B. Spatial Resolution of e^-

Using the setup described in Figure 5, we acquired various data related to the angular resolutions of the electrons. The Faraday cup signals are plotted in Figures 9 through 12. The angles referred to in these plots are measured with respect to the axis along the path of the laser. Only a portion of our experimental results have been displayed in these plots. The results were reproduced almost exactly every time we repeated the experiment at a specific angle.

Figure 9 corresponds the data taken when the FCs were 22^o with respect to the axis of the laser (any closer and the Faraday cup actually blocked the path of the laser). This figure contains a very visible negative pulse, indicating a high number of electrons in comparison to ions. It is interesting to note that the forward scatter (indicated black in the figure) is almost identical in shape to the backscatter (indicated red) other than that it is slightly bigger. The positive peak at the beginning of the signal occurs too early to be attributable to ions. Ions have large mass, and therefore do not travel fast enough to make it to be beginning of the signal. Only highly relativistic electrons should be able to reach the detector that quickly. We therefore concluded that the positive peak is probably due to photo-ionization caused by light scattered from the plasma the moment it was hit by the laser. As you can see, every plot contains this characteristic positive peak. We discarded this peak as being irrelevant to either the electrons or ions.

The signals of the Faraday cups are similar, though somewhat smaller, at a slightly bigger angle of about

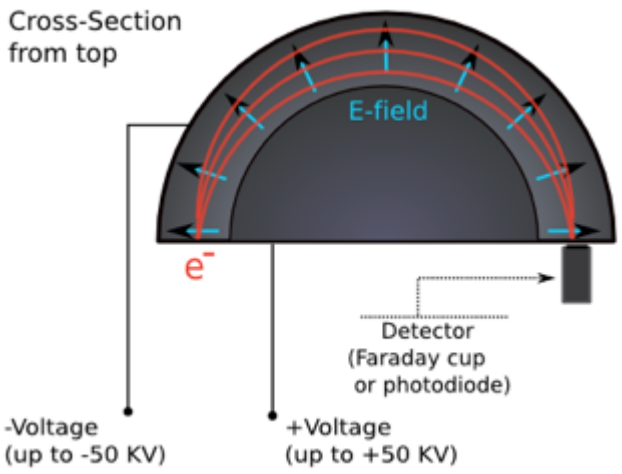

FIG. 6: This is the basic design of a Concentric Hemispherical Analyzer (CHA). It consists of two conducting hemispheres set at opposite potentials. The resulting radial field only allows electrons of a specific energy to pass all the way to the detector (a Faraday cup or photodiode) on the other side. An interesting consequence of this geometry is that the electrons are mapped exactly to the other side of the sphere.

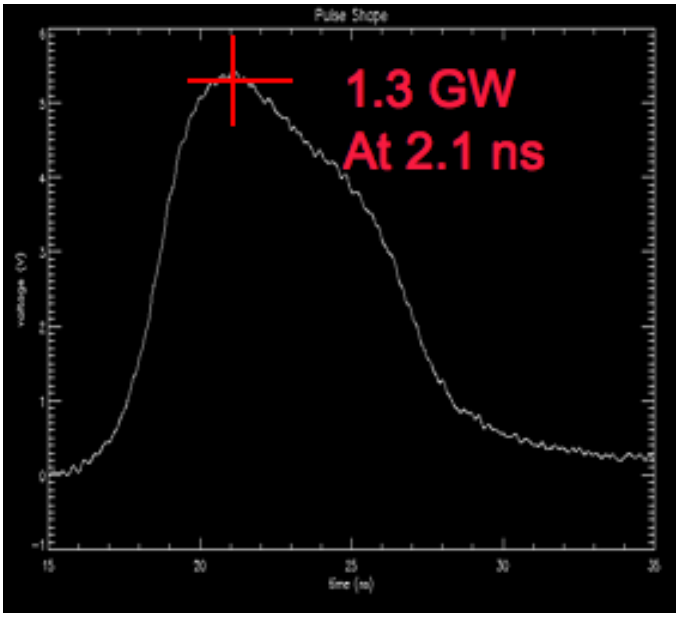

FIG. 7: This is a power-time plot for a typical shot at the PHOENIX laser. We needed to determine the maximum power in order to determine the maximum intensity. At a laser-fusion laboratory, the max-intensity point is where a fusion ignition would be expected to occur.

30^o (shown in Figure 10). The data is still indicative of a proportionally large scatter of electrons at this angle. The forward scatter and the backscatter are still similar in shape, although the discrepancy of their magnitude is more apparent. Towards the end of the signal, the voltage appears to rise to slightly above zero, showing that there were probably some (though a small number) of ions being detected. The ions (He nuclei) are much more massive than the electrons and therefore travel slower. Positive signals from ions often become significant sometime after the signal from the electrons.

There is a dramatic change in the signal at the angle of 45^o (Figure 11). At this angle the signal is actually positive during the entire time. There are proportionally a lot more positive ions being emitted at this angle than there are electrons. As noted before, ions travel slower then electrons, which explains why the positive pulse seems to peak later than the negative pulses of the previous diagrams. Note that this signal does not indicate that there are no electrons detected, but that the number of ions are overwhelmingly higher- effectively drowning any electron signal.

The signal is still positive at an angle of 60^o, but much smaller. The decrease in signal strength between 45^o and 60^o is surprisingly drastic. There is a small negative pulse, indicating that there are still a small number of electrons, detectable now that the number of ions is not sufficient to drown them. Interestingly, this decrease in signal persisted to the angle of 90^o, where there was no signal at all other than noise. Overall, the strongest signals were those of small angles, whereas the signals above 45^o were hardly significant in comparison.

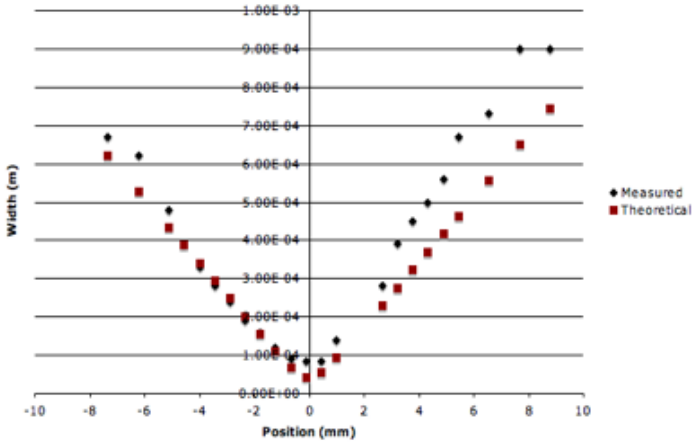

FIG. 8: This is a comparison of the experimentally-measured laser intensity and the theoretically-expected distribution. They are both plotted with respect to distance from the focal point. The experimentally-measured values are reasonable, especially around the focus.

A likely distribution of the ions and electrons emitted from the He plasma is shown in Figure 13. The forward scatter and backscatter were very similar for every angle at which we obtained data, indicating a rough symmetry about the center of rotation. Strong negative signals were detected at small angles up to 30^o. Most of the electrons are probably emitted near the axis of the laser. This makes some intuitive sense, since the laser is prone to blowing electrons towards the same direction it

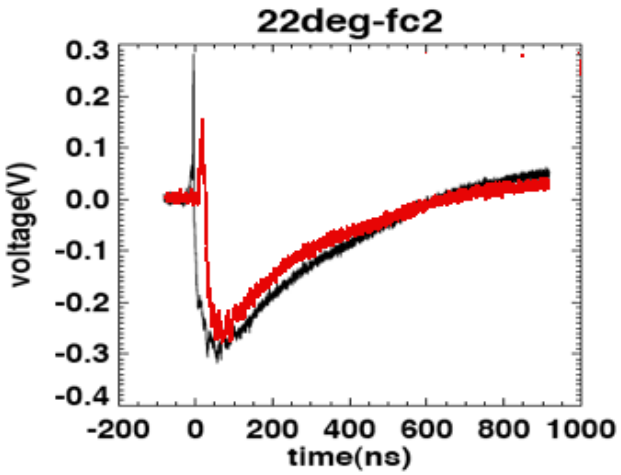

FIG. 9: These are the voltage signals acquired from Faraday cups 1 and 2 (FC1 and FC2). FC2 is located at 22^o from the axis of the laser (FC1 is located at 112^o). The FC2 data is colored black, and signifies the forward scatter signal. FC1 is colored red, and signifies the backscatter. There seems to be a symmetry between the backscatter and forward scatter at this angle. The signal is negative, implying a proportionally large number of electrons being emitted.

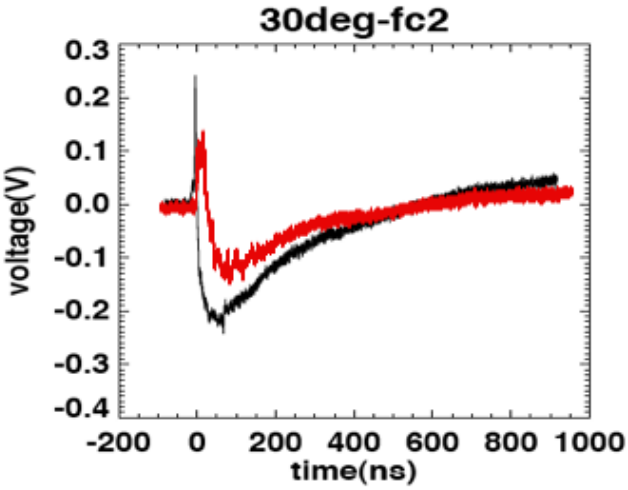

FIG. 10: These are the voltage signals acquired from Faraday cups 1 and 2 (FC1 and FC2). FC2 is located at 30^o from the axis of the laser (FC1 is located at 120^o). The FC2 data is colored black, and signifies the forward scatter signal. FC1 is colored red, and signifies the backscatter. As you can see, there seems to be a symmetry between the backscatter and forward scatter at this angle. The signal is negative, implying a proportionally large number of electrons being emitted.

is propagating. The backscatter is probably caused by electrons "bouncing back" after being compressed by the laser. Slightly larger angles indicate a greater number of ions than that of electrons. The positive signals appear slower, since ions are much more massive and therefore take more time to reach the detector. From that angle, the signal reduces significantly until it reaches zero at 90^o.

You can determine the velocity of an electron by dividing the distance from the plasma to the FC by the time of flight (obtainable from the plots). The kinetic energy of the electrons can then be obtained from the familiar relativistic equation $E_{kin} = (\gamma - 1)m_e c^2$. Using this relation, I found that the majority of the electrons in Figure 9 are at about 10 eV, with a few ranging up to 100 eV. This is not a high enough energy to be attributable to SRS, but rather to the Inverse Bremsstrahlung (which is what we expected at this laser intensity).

In this way, a Faraday cup can be used to obtain some useful insights into the spatial resolution of electrons and ions. Specifically, it was important for us to know where to place the electron spectrometer, which is much larger and difficult to adjust then the Faraday cups. If it is located at 90^o from the axis of the laser, it would probably receive no signal, whereas if it is located at as small an angle as possible, it would receive plenty of electron signals.

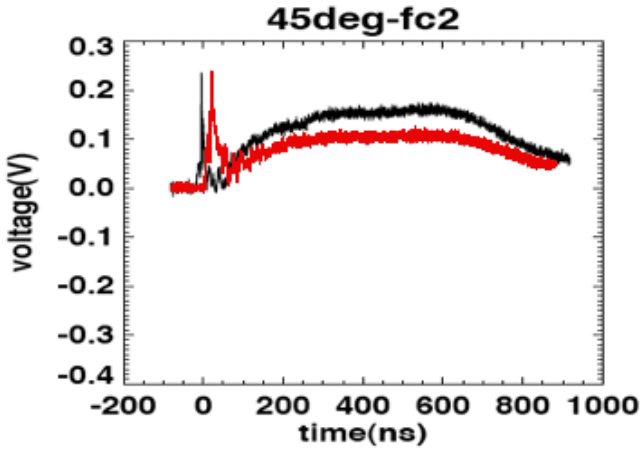

FIG. 11: These are the voltage signals acquired from Faraday cups 1 and 2 (FC1 and FC2). FC2 is located at 45^o from the axis of the laser (FC1 is located at 135^o). The FC2 data is colored black, and signifies the forward scatter signal. FC1 is colored red, and signifies the backscatter. There seems to be a symmetry between the backscatter and forward scatter at this angle. The signal is positive, signifying that there are more positive ions than electrons being emitted at this angle.

C. Electron Gun

We were able to successfully float the electron gun to a potential of $10k\Omega$ without any arching. Once we obtain a bigger high-voltage supply, we hope to test it up to $50k\Omega$. We tried to observe the emitted electrons using

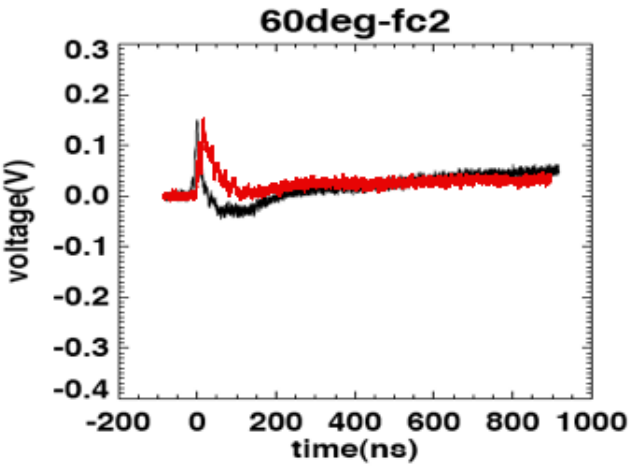

FIG. 12: These are the voltage signals acquired from Faraday cups 1 and 2 (FC1 and FC2). FC2 is located at 60^o from the axis of the laser (FC1 is located at 150^o). The FC2 data is colored black, and signifies the forward scatter signal. FC1 is colored red, and signifies the backscatter. There seems to be a symmetry between the backscatter and forward scatter at this angle. The signal is positive, signifying that there are more positive ions than electrons being emitted at this angle.

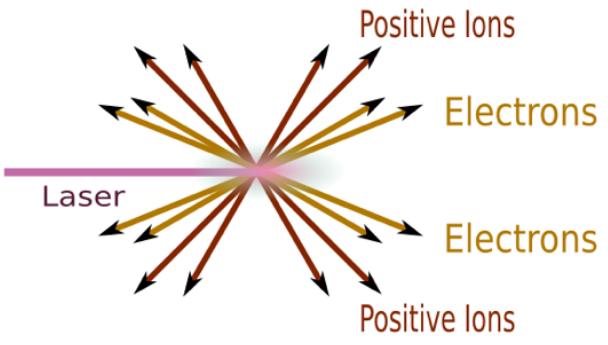

FIG. 13: A likely distribution according to the data presented in Figures 9 through 12. Very small angles 22^o through 30^o showed signals indicating a large number of elections, whereas larger angles 45^o through 60^o showed a proportionally large number of positive ions. No signal was observed at 90^o. I should note that the system is cylindrically symmetric around the axis of the laser. The distribution should likewise be cylindrically symmetric.

a Faraday cup (a photodiode is not as sensitive), but did not detect a significant signal. In order to use the electron gun to calibrate the CHA, we therefore need a more intense beam of electrons.

There are various ways that we could hope to improve the electron beam intensity. One problem in the design of the gun is apparent from Figure 15. The filament produces a semi-radial potential field. The electrons which are emitted radially are then attracted by the grounded plate and redirected to a straighter path. A consequence of this is that many of the electrons approach the plate on a curved path, and miss the hole entirely. The potential field may be made more uniform by introducing a plate behind the filament, and at the same high negative voltage. A more uniform potential field will allow the electrons to follow a straighter path to the plate, allowing for more electrons to make it through the hole, contributing to the beam.

Another way to increase the electron beam intensity would be to use a higher power of lamp-filament. This would require some way of introducing more batteries to the circuit, and probably some replacement of resistors to adjust the current to what is appropriate for the new lamp. A lamp with a higher wattage will reach a higher temperature, and will also have a greater surface area with which to radiate electrons. An electron multiplier tube could also be used to increase the intensity even further.

We were not able to calibrate the CHA while I was at UCLA (the power supply for the CHA had not arrived yet). It should be simple to adjust the electron gun to get a strong enough source of electrons once the spectrometer is ready to be calibrated.

V. CONCLUSION

We made great progress in the development and testing of hot electron detectors. We successfully built a couple Faraday cups. We were then able to use them to obtain reproducible data on the angular resolution of the electrons from an He plasma. The Faraday cups also gave a very rough idea of the electron energies, which we found ranged at least up to 100 eV. The electron gun we built seems to handle voltages at least up to 10 kV without any complications. At this point the electron beam is too small to be useful for calibration. This problem can be solved by changing the light-bulb filament, evening the potential field with a conducting plate, or placing an electron multiplier in the path of the beam. We could not test the CHA while I was at UCLA (we did not yet have the power supply), but when it is ready, the electron gun may be used to determine the proportionality

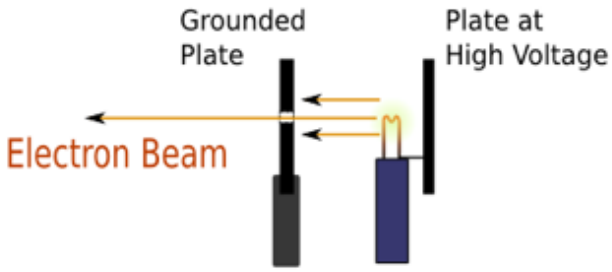

FIG. 14: A uniform potential field may help let more electrons contribute to the final beam.

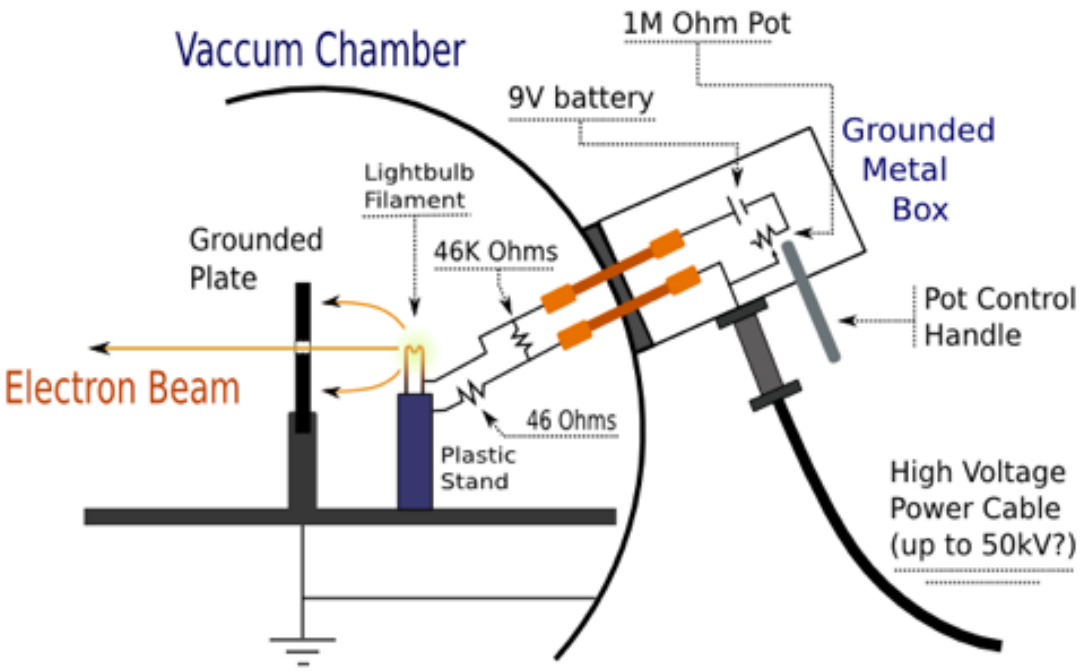

FIG. 15: This is the general design of the electron gun, to be used for calibrating the electron spectrometer in Figure 6. It is effectively a 9V light-bulb circuit floating at a high negative potential. The electrons are boiled off as the filament acquire heat, and then repelled by its negative potential. The electrons are then attracted to the grounded plate. The ones that make it through the hole in the plate produce a beam of electrons, with energy specified by the potential at which the filament was floating. The main challenge was to build the equipment to handle high-voltage without the risk of arching.

between the applied potential and the energy of the detected electrons.

Unfortunately, while I was at the PHOENIX facility, the laser intensity was not sufficient to produce electrons from a SRS laser-plasma instability. This problem was fixed (the broken capacitor replaced) after I left. The Faraday cups and the CHA will then be useful for observing the temporal, spatial, and spectral resolution of the SRS. The understanding of Stimulated Raman Scattering will be crucial for the future success of inertial confinement fusion.

VI. ACKNOWLEDGEMENTS

I thank Christoph Niemann (my mentor), and Carmen Constantin for guiding me and helping me through my time at UCLA. I also thank Erik Everson, a graduate student working on a similar project, for helping me and supporting me though my research. I thank Francoise Queval for managing and organizing the internship. Finally, I thank NSF for the financial support that made it possible for me to pursue research as an undergraduate this summer.

[1] C. S. et al., Rev. Scientific Instruments **72**, 1197 (2001).
[2] J. W. M. et al., Physics of Plasmas **13**, 2006 (2006).
[3] S. WIlks and W. Kruer, Journal of Quantum Electronics **33**, 1954 (1997).
[4] F. et al., Phys. Rev. A. **11**, 679 (1975).
[5] W. Kruer, Physics of Plasmas **10**, 2087 (2003).